Dominant electronic oscillators in the optical nonlinearities of conjugated polyenes

Guanhua Chen, Shaul Mukamel

Center for Photoinduced Charge Transfer, Department of Chemistry, University of Rochester, Rochester, NY 14627, USA

Received 22 February 1995; in final form 2 May 1995

Abstract

In the coupled-oscillator representation [Takahashi and Mukamel, J. Chem. Phys. 100 (1994) 2366], the optical properties of conjugated polymers are calculated by mapping the system into a collection of coupled normal modes representing electron-hole pairs. Optical nonlinearities are induced by anharmonic couplings among oscillators and with the external field. Tree diagrams are developed which visualize the relevant nonlinearities and dominant oscillators and provide an efficient algorithm for computing the hyperpolarizabilities.

1. Introduction

The sum-over-state method is commonly used in quantum chemical calculations of optical susceptibilities [1-6]. The optical properties are then related to the eigenvalues and dipole matrix elements of the global many-electron eigenstates, and physical intuition is developed through the properties of the ground and the excited states. Recently a fundamentally different approach, the coupled-oscillator picture, has been developed to investigate optical properties of conjugated polymers [7-11]. It relates the electronic charges and motions directly to the optical response, without introducing the global eigenstates. This greatly reduces the computational effort. The electronic degrees of freedom are modeled as a collection of harmonic oscillators, and the nonlinear response arises from anharmonic couplings among oscillators and couplings between oscillators and the external field. In previous studies [7,9,10], very few dominant oscillators, typically 1-10, have been found for the optical responses in large conjugated polymers, out of

the total number of oscillators $M = N(N + 1)/2$, N being the number of carbon atoms. In this Letter, we illustrate how to identify these dominant oscillators and anharmonicities. Basing on this, we will build a simple intuitive picture of optical processes in conjugated polyenes, and propose an efficient algorithm to calculate hyperpolarizabilities.

The method we employ is the time-dependent Hartree-Fock (TDHF). The TDHF describes quantum fluctuation around the Hartree-Fock ground state. It therefore takes into account some important correlation effects, and goes beyond the normal Hartree-Fock procedure [12-14]. We have demonstrated that it can reproduce some key nonlinear optical properties of conjugated polymers [7,9-11]. We first solve for the Hartree-Fock ground state with geometry optimization, and then calculate the density matrix to first, second and third orders in the external field. Details of the method were given previously [7,10].

We will focus on the off-resonant polarizabilities of a relatively small system, octatetraene [15]. Our starting point is the PPP Hamiltonian which is based

on the Su–Schrieffer–Heeger (SSH) tight binding Hamiltonian with the addition of Coulomb interaction [7,10,16,17]. We follow the dynamics of the single electron reduced density matrix $\rho_{nm}(t) = \langle c_m^+ c_n \rangle$, where c_m^+ (c_m) is the creation (annihilation) operator for a π electron at site m [7,10,18–21]. A system of N atoms is mapped into a collection of M oscillators with frequencies Ω_ν. These include N zero frequency oscillators. Each oscillator ν has a coordinate $\hat{Q}_\nu$ and a momentum $\hat{P}_\nu$. By expanding the density matrix in these oscillators we obtain $\delta\rho_{nm}(t) \equiv \rho_{nm}(t) - \rho_{nm}^{(0)} = \sum_\nu Q_\nu(t)\hat{Q}_\nu + P_\nu(t)\hat{P}_\nu$, where $\rho^{(0)}$ is the reduced Hartree–Fock ground state density matrix, and $Q_\nu(t)$ and $P_\nu(t)$ are time-dependent coefficients. For the static response (setting the optical frequency is zero) we have $P_\nu = 0$.

The nth order polarization can be calculated using the following expression:

$$P^{(n)} = \sum_\nu d_\nu Q_\nu^{(n)}, \qquad (1)$$

where $Q_\nu^{(n)}$ represent the amplitude of the νth harmonic oscillator with frequency Ω_ν to nth order in the field and dipole moment d_ν,

$$d_\nu = -\sum_m 2\sqrt{2}\, ez(m)\mathcal{U}_{mm,\nu}^{-1}, \qquad (2)$$

where $z(m)$ is the coordinate of mth atom in the chain direction and $\mathcal{U}_{mn,\nu}^{-1}$ is the mn component of eigenvector for an oscillator ν. The nth order polarizability χ_n is given by [10]

$$\chi_n = \sum_\nu d_\nu Q_\nu^{(n)}/\mathcal{E}^n, \qquad (3)$$

where $\chi_1 = \alpha$, $\chi_2 = \beta$, $\chi_3 = \gamma$, and $\mathcal{E}$ is the external field.

The oscillator amplitudes $Q_\nu^{(n)}$ are calculated successively, order by order in the field $\mathcal{E}$. According to Ref. [10], for nonzero frequency modes ($\Omega_\nu \neq 0$),

$$Q_\nu^{(1)} = \frac{1}{\Omega_\nu}\bar{E}_\nu \mathcal{E},$$

$$Q_\nu^{(2)} = -\frac{1}{\Omega_\nu}\sum_{\nu'} D_{\nu,\nu'}^{a} Q_{\nu'}^{(1)} \mathcal{E}$$

$$-\frac{1}{\Omega_\nu}\sum_{\nu'\nu''}(C_{\nu,\nu'\nu''}^{a} + X_{\nu,\nu'\nu''}^{a})Q_{\nu'}^{(1)}Q_{\nu''}^{(1)},$$

$$Q_\nu^{(3)} = -\frac{1}{\Omega_\nu}\sum_{\nu'} D_{\nu,\nu'}^{a} Q_{\nu'}^{(2)} \mathcal{E}$$

$$-\frac{1}{\Omega_\nu}\sum_{\nu'\nu''}(C_{\nu,\nu'\nu''}^{a} + X_{\nu,\nu'\nu''}^{a})Q_{\nu'}^{(1)}Q_{\nu''}^{(2)}. \qquad (4)$$

For centrosymmetric systems, the zero frequency modes ($\Omega_\mu = 0$) give,

$$Q_\mu^{(1)} = Q_\mu^{(3)} = 0,$$

$$Q_\mu^{(2)} = \sum_{\nu'} \frac{1}{2\Omega_\nu'} D_{\mu,\nu'}^{b} Q_{\nu'}^{(1)} \mathcal{E}$$

$$+\sum_{\nu'\nu''}\frac{1}{2\Omega_\nu''}(C_{\mu,\nu'\nu''}^{b} + X_{\mu,\nu'\nu''}^{b})Q_{\nu'}^{(1)}Q_{\nu''}^{(1)}. \qquad (5)$$

Here $\bar{E}_\nu$ represents linear coupling of an oscillator ν to the driving field. $D_{\nu,\nu'}$ stands for the coupling between oscillators ν and ν' through the external field. $C_{\nu,\nu'\nu''}$ represents anharmonic couplings among oscillators resulting from Coulomb interactions whereas $X_{\nu,\nu'\nu''}$ are additional anharmonicities related to exchange interactions. All of these coefficients can be expressed in terms of the original parameters of the Hamiltonian, and the ground state reduced density matrix $\rho^{(0)}$ [10].

2. Oscillator analysis of the optical response

2.1. Electronic normal modes

Octatetraene has 28 finite frequency oscillators and 8 zero frequency oscillators. Since the molecule is centrosymmetric, these oscillators are either symmetric (A_g) or antisymmetric (B_u). Table 1 lists the frequencies, dipole moments and oscillator strengths for all oscillators. We found 20 A_g oscillators and 16 B_u oscillators. The A_g oscillators have zero dipole moments and zero oscillator strengths, and do not couple directly with the external field. They do affect however the optical nonlinearities since they are anharmonically coupled to the B_u oscillators. The majority of B_u oscillator have nonzero dipole moments and couple to the external field.

We shall examine the contribution of each oscillator to the density matrix ρ in different orders. The nth order density matrix $\delta\rho^{(n)}$ can be expressed as $\delta\rho^{(n)} = \sum_\nu Q_\nu^{(n)}|\hat{Q}_\nu\rangle\rangle$. Table 2 lists $|Q_\nu^{(n)}|$ to first, second and

Table 1
Properties of the A_g and B_u electronic harmonic oscillators[a]

A_g	(1)	(2)	(3)	(4)	(5)	(6)	(7)	(8)
Ω_ν	0	0	0	0	0	0	0	0
A_g	(9)	(10)	(11)	(12)	(13)	(14)	(15)	(16)
Ω_ν	2.677	2.677	3.555	3.555	5.739	6.064	7.604	7.980
A_g	(17)	(18)	(19)	(20)				
Ω_ν	9.131	9.964	11.290	12.847				
B_u	(1)	(2)	(3)	(4)	(5)	(6)	(7)	(8)
Ω_ν	1.047	1.047	1.630	1.630	1.925	1.925	4.034	4.602
d_ν	2.370	2.370	2.725	2.725	2.773	2.773	2.657	0.003
f_ν	0	0	0	0	0	0	7.351	0
B_u	(9)	(10)	(11)	(12)	(13)	(14)	(15)	(16)
Ω_ν	4.602	6.932	7.301	8.166	9.452	10.745	10.988	13.025
d_ν	0.003	0.534	0	0.217	0.110	0	0.055	0.002
f_ν	0	0.512	0	0.098	0.031	0	0.008	0.0

[a] For A_g oscillator, $d_\nu = 0$ and $f_\nu = 0$, Ω_ν is in the units of eV, and d_ν is in the units of e Å.

Table 2
Amplitudes of oscillators $|Q_\nu^{(n)}|$ in first, second and third order

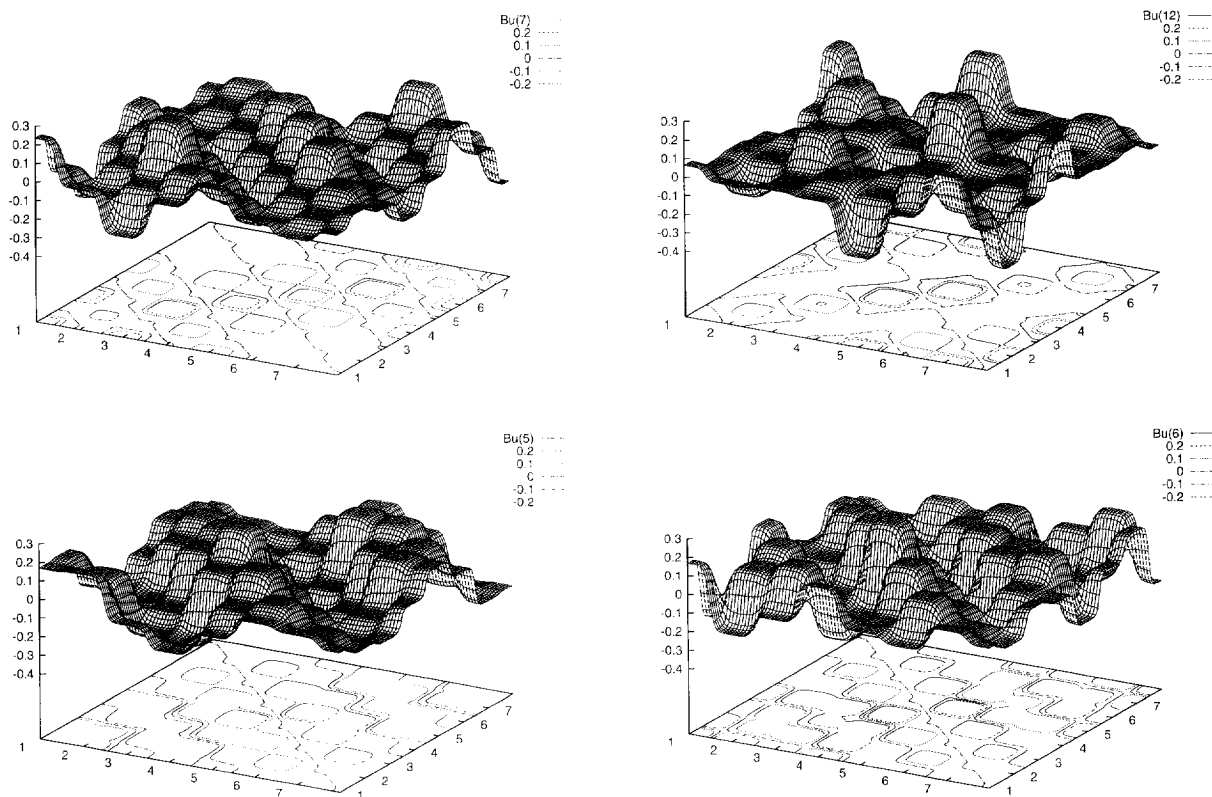| B_u	(7)	(10)	(12)	(13)	(15)	(16)
$|Q_\nu^{(1)}|$	4.70×10^{-1}	5.53×10^{-2}	1.88×10^{-2}	8.25×10^{-3}	3.51×10^{-3}	8.78×10^{-5}
A_g	(14)	(1)	(2)	(16)	(3)	(4)
$|Q_\nu^{(2)}|$	1.13×10^{-1}	6.60×10^{-2}	6.60×10^{-2}	1.55×10^{-2}	5.15×10^{-3}	5.15×10^{-3}
A_g	(11)	(12)	(18)	(5)	(6)	(9)
$|Q_\nu^{(2)}|$	3.87×10^{-3}	3.87×10^{-3}	3.09×10^{-3}	6.24×10^{-4}	6.24×10^{-4}	4.36×10^{-4}
A_g	(10)	(20)	(7)	(8)		
$|Q_\nu^{(2)}|$	4.36×10^{-4}	4.33×10^{-4}	7.65×10^{-5}	7.65×10^{-5}		
B_u	(12)	(5)	(6)	(7)	(13)	(15)
$|Q_\nu^{(3)}|$	3.22×10^{-2}	2.22×10^{-2}	2.22×10^{-2}	1.86×10^{-2}	5.63×10^{-3}	2.80×10^{-3}
B_u	(3)	(4)	(8)	(9)	(1)	(2)
$|Q_\nu^{(3)}|$	2.47×10^{-3}	2.47×10^{-3}	1.47×10^{-3}	1.47×10^{-3}	3.43×10^{-4}	3.43×10^{-4}
B_u	(10)	(16)				
$|Q_\nu^{(3)}|$	2.84×10^{-4}	8.43×10^{-5}				

Fig. 1. The density matrices of B_u oscillators for octatetraene. The density matrix is an 8×8 matrix. The top is a continuous surface representing B_u oscillator, and the bottom is a contour representation.

third order ($n = 1, 2, 3$). In the calculation, the magnitude of electric field is assumed to be 1 V/Å. Selection rules imply that the first and third order solutions contain only B_u oscillators and in second order, there are only A_g oscillators [7].

2.2. Dominant oscillators

As is evident from Table 2, only few oscillators dominate in each order. In first order, there is one dominant oscillator $B_u(7)$, which will be denoted the absorption mode (AM). In Fig. 1 we plot the density matrix representing the eigenvector $\hat{Q}_\nu$ of this mode. The diagonal elements ρ_{nn} represent the charge at site n. Since electrons move across the π bond, we find that the elements parallel to the anti-diagonal line polarize in the same way. Thus, the density matrix elements form alternating arrays of hills and valleys parallel to the anti-diagonal direction ($n - m$ is varied with $n + m$ held fixed). The three dominant oscillators in second order are displayed in Fig. 2. These include two

zero frequency modes (ZFM), $A_g(1)$ and $A_g(2)$. In third order, there are three dominant oscillators $B_u(5)$, $B_u(6)$ and $B_u(12)$ in addition to AM. Their density matrices are shown in Fig. 1 as well. Oscillators $B_u(5)$ and $B_u(6)$ form alternating hills and valleys along the anti-diagonal direction similar to AM. The diagonal elements of $B_u(12)$ also form a similar pattern.

To further explore the nature of these dominant oscillators, we shall study their composition. In Ref. [10], in addition to the real space site representation, we introduced the Hartree–Fock oscillator (HFO) representation. In this representation, each HFO $[q_1, q_2]$ is connected to the transition among two Hartree–Fock molecular orbitals q_1 and q_2. Projecting oscillators onto HFO space connects electronic harmonic oscillators with the molecular orbitals. In Fig. 3, we plot the HFO components of the dominant oscillators. Based on these observations, the dominant oscillators can be constructed by a simple algorithm, which will be discussed below.
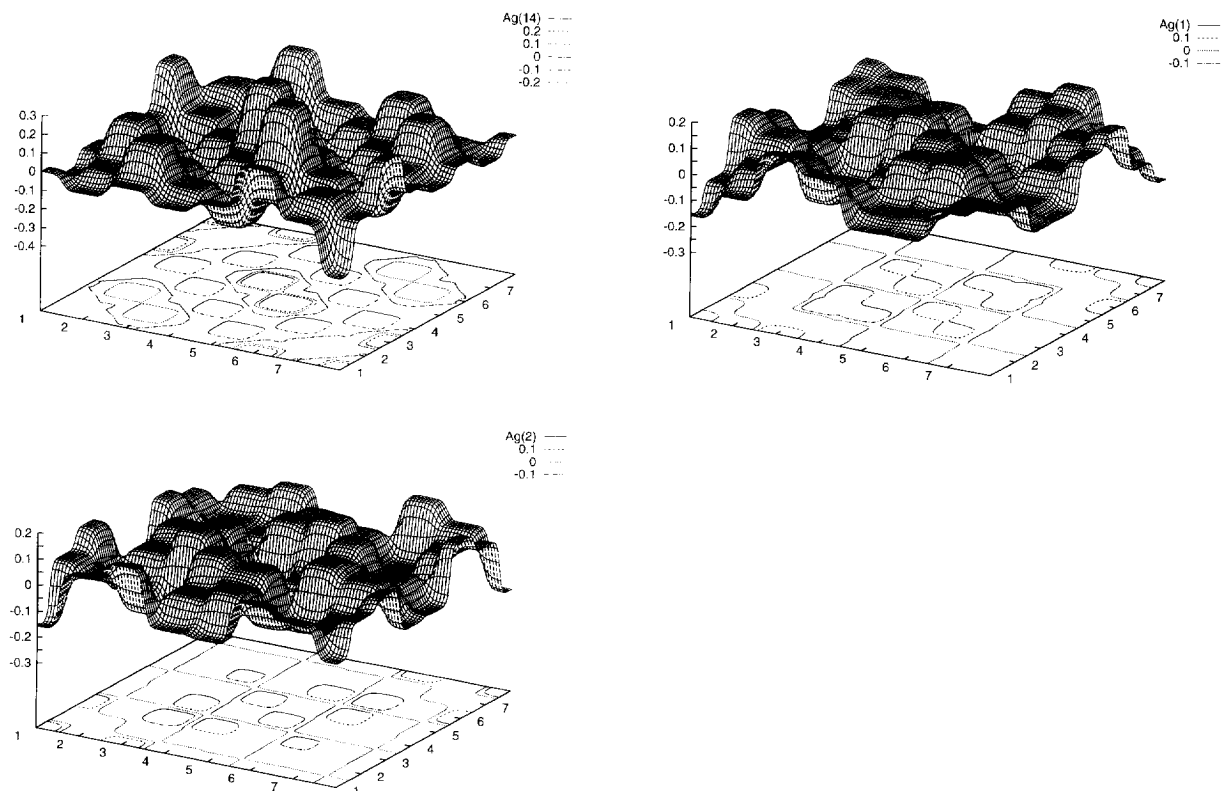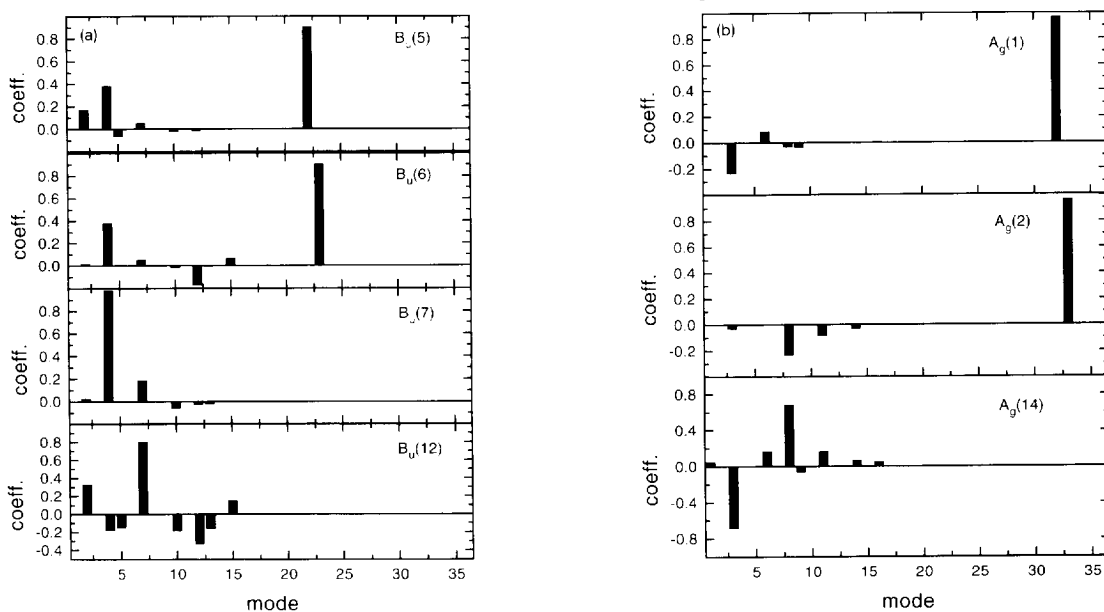
Fig. 2. The same as Fig. 1 but for the A_g oscillators.

Fig. 3. Projections of dominant oscillators onto the Hartree–Fock oscillator (HFO) representation. (a) B_u oscillators: $B_u(7)$ (AM) is made primarily of $[p_1h_4]$, $B_u(5)$ $[B_u(6)]$ made of $[p_1p_2]$ and $[p_1h_4]$ ($[h_3h_4]$ and $[p_1h_4]$), and $B_u(12)$ is made of mainly $[p_2h_3]$. (b) A_g oscillators: $A_g(1)$ $[A_g(2)]$ (ZFM) are made mainly of $[p_1p_1]$ and $[p_1h_4]$ ($[h_4h_4]$ and $[p_1h_4]$), and $A_g(14)$ is made of $[p_1h_3]$ and $[p_2h_4]$.

Table 3
Percentages of dominant nonlinear coupling parameters D, C and X

	4	6	8	10	12	14	16
$D_{\nu,\nu'}$	20.0	12.2	8.33	5.85	5.08	4.02	3.35
$C_{\nu,\nu'\nu''}$	15.3	7.23	3.84	2.23	1.52	0.97	0.59
$X_{\nu,\nu'\nu''}$	11.9	4.82	2.08	0.97	0.50	0.32	0.14

2.3. Dominant nonlinearities

In the coupled-oscillator picture, harmonic oscillators interact with the the field and with each other through the coupling parameters D, C and X. Thus, it is important to examine these parameters. The total number of $D_{\nu,\nu'}$, $C_{\nu,\nu'\nu''}$ and $X_{\nu,\nu'\nu''}$ coefficients is M^2, M^3 and M^3, respectively. In Fig. 4, we plot the histograms for the absolute magnitudes of $\bar{E}_\nu$, $D_{\nu,\nu'}$, $C_{\nu,\nu'\nu''}$ and $X_{\nu,\nu'\nu''}$. Most of them are very small and can be neglected. Only a tiny fraction of $D_{\nu,\nu'}$, $C_{\nu,\nu'\nu''}$ and $X_{\nu,\nu'\nu''}$ contribute to optical response, and they can be determined by introducing some cut-off. In Table 3, we list the percentages of dominant $D_{\nu,\nu'}$, $C_{\nu,\nu'\nu''}$ and $X_{\nu,\nu'\nu''}$ with absolute magnitudes greater than 0.7 (in units of e Å $\hbar^{-1}$) for different molecular sizes, $N = 4$, 6, 8, 10 and 12. For $N = 8$, the percentages for D, C and X are 6.48, 2.17 and 0.55, respectively. Other D, C and X are much smaller. This illustrates why there are only few dominant oscillators. Basing on this observation, we developed the following procedure to calculate hyperpolarizabilities. We first determine the dominant oscillators $\{\nu\}$ in first order using the criteria $|\bar{E}_\nu| > 0.7$. We next calculate D_{μ',ν_1}, $C_{\mu',\nu_1\nu_2}$ and $X_{\mu',\nu_1\nu_2}$, where $\nu_1, \nu_2 \in \{\nu\}$, keep only those with absolute value larger than a certain cut-off (chosen to be 0.7). This should identify the dominant oscillators $\{\mu\}$ in second order. Finally we calculate $D_{\lambda',\mu'}$, $C_{\lambda',\nu'\mu'}$ and $X_{\lambda',\nu'\mu'}$ where $\nu' \in \{\nu\}$ and $\mu' \in \{\mu\}$, again keeping only those greater than our chosen cut-off, and obtain the third order dominant oscillators.

We used this procedure to calculate the off-resonant polarizabilities $\alpha(0)$, $\beta(0)$ and $\gamma(0)$ of octatetraene. The resulting values of $\alpha(0)$ and $\gamma(0)$ are 1.77 e Å^2 V^{-1} and 0.267 e Å^3 V^{-2}, respectively. Compared with the values obtained by retaining all 36 oscillators $\alpha(0) = 1.81$ e Å^2 V^{-1} and $\gamma(0) = 0.255$ e Å^3 V^{-2}, the relative errors are 2.7% and 4.9%, respectively.
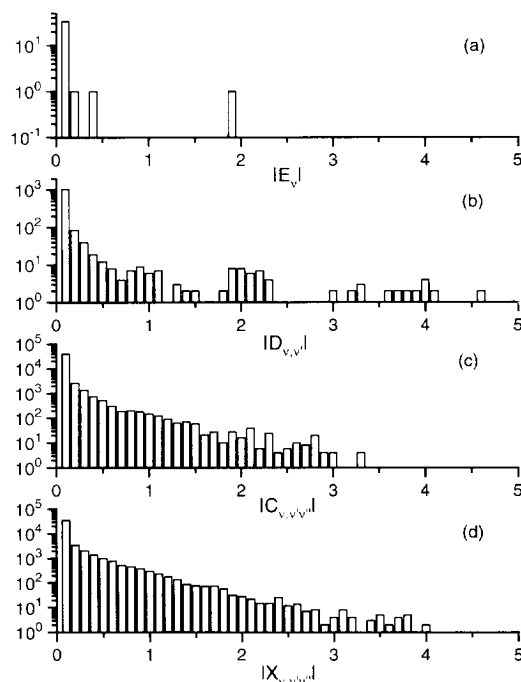

Fig. 4. Histograms for the absolute magnitudes of harmonic and anharmonic couplings. (a) Harmonic coupling $\bar{E}_\nu$; (b) anharmonic coupling $D_{\nu,\nu'}$; (c) $C_{\nu,\nu'\nu''}$; (d) $X_{\nu,\nu'\nu''}$.

2.4. Tree diagrams for dominant oscillators

In Section 2.3, we outlined a procedure to identify the dominant oscillators and calculate $\alpha(0)$, $\beta(0)$ and $\gamma(0)$ by introducing a cut-off for D, C and X associated with the dominant oscillators in lower orders. This procedure shows how the oscillators couple successively. In first order, the external field couples with the first order dominant oscillators; in second order, the first order dominant oscillators couple with the external field and among themselves to produce the second order oscillators; and in third order, the second order oscillators couple with the external field and with the first order oscillators to produce third order oscil-
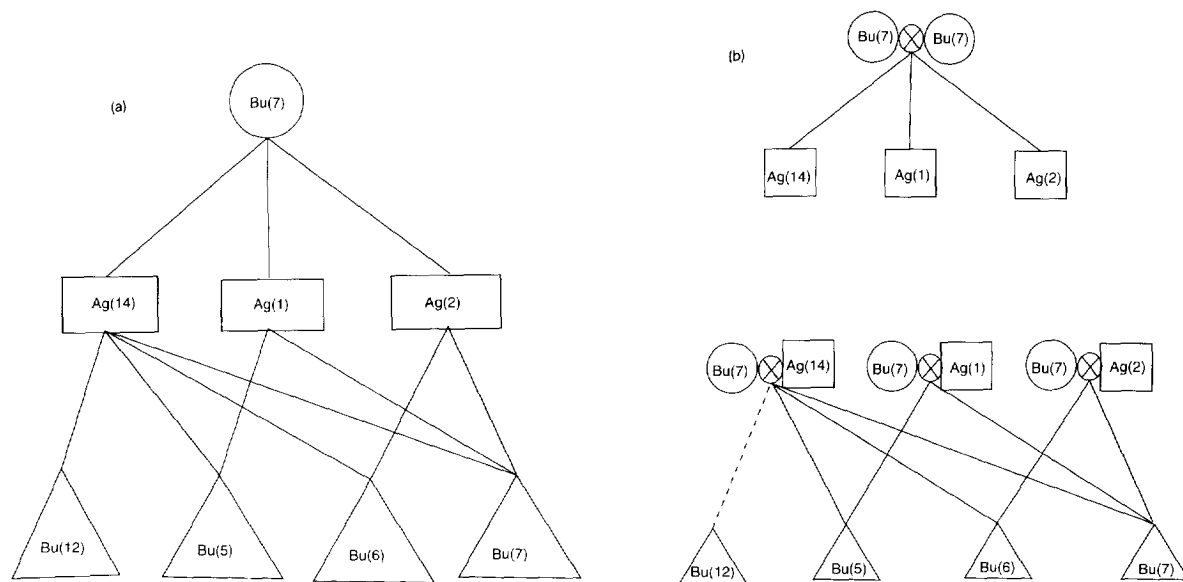
Fig. 5. (a) Tree diagram for the anharmonic coupling $D_{\nu,\nu'}$. Circles, triangles and squares represent the first, second and third order dominant oscillators, respectively. The lines stand for the $D_{\nu,\nu'}$ couplings. (b) Tree diagrams for the anharmonic coupling $C_{\nu,\nu'\nu''}$ and $X_{\nu,\nu'\nu''}$. Circles, triangles and squares represent the first, second and third order dominant oscillators, respectively. The solid lines stand for the $C_{\nu,\nu'\nu''}$ and $X_{\nu,\nu'\nu''}$ couplings and the dashed line stands for $C_{\nu,\nu'\nu''}$ only. $\otimes$ means the product of two oscillators.

lators. To illustrate this mechanism, we introduce tree diagrams in which circles, squares and triangles represent dominant oscillators in first, second and third orders respectively, and lines represent nonlinear couplings. In Fig. 5a, we show a tree diagram representing the couplings D between the dominant oscillators and the external field, and Fig. 5b gives the tree diagrams for the couplings C and X. The dotted line indicates C couplings only while solid lines represent both C and X couplings. Since these represent anharmonic couplings among oscillators, two oscillators are required to produce each third order oscillator. Thus, the tree diagrams in Fig. 5b are different from Fig. 5a. In each order (second and third), it starts with products of two dominant oscillators and produces oscillators of next order (Fig. 5b). The tree diagrams provide a clear view of nonlinear optical properties. Instead of transitions among eigenstates, nonlinear optical processes are related to a hierarchy of successively coupled oscillators. Figs. 5a and 5b illustrate that starting with the AM, these couplings produce three second order oscillators and subsequently four third order oscillators. There are only three D couplings, three C and three X couplings involved in the second order process. In addition, there are eight D, eight C and seven

X involved in the third order process. Compared with the total number of possible different couplings (36^2 for D, 36^3 for C and X), this is a great simplification of the anharmonic coupling picture.

3. Discussion

We have identified seven dominant oscillators. AM is the only oscillator in first order, and is excited by the external field interacting with the ground state. All other oscillators in second and third orders are linked to AM. Therefore, it is important to explore the nature of the AM. Although we only investigated octatetraene, we expect the following features of AM to hold for larger polyenes as well, (1) π electrons polarize at double bond sites and electrons move across double bonds; (2) the AM density matrix forms arrays of hills and valleys alternating along the diagonal direction; (3) for an even numbered conjugated polymer, $[Q_{AM}]_{nm} = 0$ when $n+m$ is odd. AM is primarily made of the HOMO/LUMO transition. Thus, AM is readily constructed. As shown in Section 2.2, other dominant oscillators are all made of the first two HOMO and LUMO. This implies that we only

need a few molecular orbitals near the Fermi level to construct the dominant oscillators. As the system size increases, intervals between adjacent levels decrease and the number of molecular orbitals near the Fermi surface increase.

The primary goal of this Letter is to develop an intuitive and systematic picture of dominant oscillators. Tree diagrams represent the dynamics of dominant oscillators and provide an alternative to the essential states picture [22]. For centrosymmetric systems, a selection rule which is based on the symmetry of oscillators states that in the first and third orders only B_u oscillators appear while in the second order only A_g oscillators contribute. However, $B_u(11)$ and $B_u(14)$, and $A_g(13)$, $A_g(15)$, $A_g(17)$ and $A_g(19)$ do not appear in any order. Upon inspection of these oscillators, we found that (1) for $B_u(11)$ and $B_u(14)$, $\rho_{nm} = 0$ when $n + m$ is even while for others B_u oscillators $\rho_{nm} = 0$ when $n + m$ is odd; (2) for $A_g(13)$, $A_g(15)$, $A_g(17)$ and $A_g(19)$, $\rho_{nm} = 0$ when $n + m$ is odd while $\rho_{nm} = 0$ when $n + m$ is even for other A_g oscillators.

In summary, the anharmonic coupling parameters of octatetraene show that only a very small faction contributes to the polarizabilities. Based on this observation, we introduced tree diagrams to represent the anharmonic couplings, illustrate the emergence of dominant oscillators and thus explain the origins of nonlinearities. The tree diagrams provide an intuitive picture of nonlinear electronic dynamics in the system.

Acknowledgement

References

[1] B.J. Orr and J.F. Ward, Mol. Phys. 20 (1971) 513.

[2] D.S. Chemla and J. Zyss, Nonlinear optical properties of organic molecules and crystals (Academic Press, New York, 1987).

[3] D.C. Rodenberger, J.R. Heflin and A.F. Garito, Nature 359 (1992) 309.

[4] S. Etemad and Z.G. Soos, Spectroscopy of advanced materials, eds. R.J.H. Clark and R.E. Hester (Wiley, New York, 1991) p. 87.

[5] Z.G. Soos, S. Ramasesha, D.S. Galvao and S. Etemad, Phys. Rev. B 47 (1993) 1742.

[6] J.M. André, J. Delhalle and J.L. Brédas, Quantum chemistry aided design of organic polymers. An introduction to the quantum chemistry of polymers and its applications (World Scientific, Singapore, 1991).

[7] A. Takahashi and S. Mukamel, J. Chem. Phys. 100 (1994) 2366.

[8] S. Mukamel and H.X. Wang, Phys. Rev. Letters 69 (1992) 65.

[9] S. Mukamel, A. Takahashi, H.X. Wang and G. Chen, Science 266 (1994) 251.

[10] G. Chen and S. Mukamel, J. Am. Chem. Soc., in press.

[11] G. Chen, A. Takahashi and S. Mukamel, Proc. SPIE 2143 (1994) 142.

[12] D.J. Rowe, Rev. Mod. Phys. 40 (1968) 153.

[13] P. Ring and O. Schuck, The nuclear many-body problem (Springer, New York, 1980).

[14] H. Sekino and R.J. Bartlett, J. Chem. Phys. 85 (1986) 976.

[15] W.J. Buma, B.E. Kohler and T.A. Shaler, J. Chem. Phys. 96 (1992) 399.

[16] J. Linderberg and Y. Ohrn, Propagators in quantum chemistry (Academic Press, New York, 1973).

[17] H. Fukutome, J. Mol. Struct. THEOCHEM 188 (1989) 337, and references therein.

[18] U. Fano, Rev. Mod. Phys. 29 (1957) 74.

[19] R. Zwanzig, Lect. Theoret. Phys. 3 (1961) 106.

[20] R. Zwanzig, Physica 30 (1964) 1109.

[21] E.R. Davidson, Reduced density matrices in quantum chemistry (Academic Press, New York, 1976).

[22] D. Guo, S. Mazumdar, G.I. Stegeman, M. Cha, D. Neher, S. Aramaki, W.E. Torruellas and R. Zanoni, Mat. Res. Soc. Symp. Proc. 247 (1992) 151.